A Tiny Quadrotor Platform for Micro Sensor Testing and Control Design

Alyssa Michelle Giedd

A thesis

submitted in partial fulfillment of the

requirements for the degree of

Master of Science in Mechanical Engineering

University of Washington
2024

Committee:
Sawyer Fuller
Vikram Iyer
Santosh Devasia

Program Authorized to Offer Degree:
Mechanical Engineering

University of Washington

Abstract

A Tiny Quadrotor Platform for Micro Sensor Testing and Control Design

Alyssa Michelle Giedd

Chair of the Supervisory Committee:

Sawyer Fuller
Mechanical Engineering

Key limitations of small hovering drones are a battery life of <30 minutes, and their impact hazard for humans. Two aspects of scaling physics mean these challenges can be mitigated by reducing their scale to just a few grams. First, low weight eliminates impact hazard. Secondly, favorable surface area-to-volume ratio may allow very small robots to fly indefinitely in direct sunlight. The smallest aircraft demonstrating autonomous hovering flight to date weighs approximately 30 grams, too heavy to realize these advantages. In this thesis we present an approach to allow for fabrication of a quadrotor weighing more than an order of magnitude less, at less than three grams. This is small enough to replicate the behavior and constraints of lightweight flying insect robots, which are an order of magnitude lighter. We implemented a novel laser-micromachined carbon fiber airframe and circuit fabrication process, origami-inspired design techniques, and have in-hand a lightweight avionics system to allow for onboard computation to achieve stable hovering flight. We show the smallest available lithium polymer battery provides sufficient current to support liftoff. Together, these advances indicate that all elements have been validated to achieve the desired objective of autonomous flight of a quadcopter weighing less than three grams. This additionally suggests untethered flight, which has not been previously accomplished at this scale on a quadrotor platform. Our system (TinyQuad) has a final mass is 2.71 grams and it demonstrates a possible thrust of approximately 3 grams. The development of this lightweight quadrotor platform will allow for future testing of lightweight sensors, power methods, and novel forms of control which are only possible onboard lightweight flying robots.

Acknowledgements

I would like to thank my committee members Sawyer Fuller, Vikram Iyer, and Santosh Devasia for serving on my committee. I would especially like to thank my advisor Professor Sawyer Fuller for his constant and unwavering support throughout my research progress. His insights and patience allowed me to explore my reseach queries to the fullest. His commitment to fostering a comfortable and inclusive working environment helped me perform my best work.

I would also like to thank my labmates for answering my many questions and building a foundation for my work. I'd especially like to thank Yash Talwekar for his commitment to developing the lightweight bluetooth sensor suite the quadcopter will eventually utilize.

I'd like to thank my friends for being the best emotional support I could ask for. Whether a session of studying or of Dungeons and Dragons, their presence and upbeat attitude helped me persevere through my toughest roadblocks.

I'd also like to thank my family for shaping me into the person I am today and driving me to pursue this degree. From my parents to my distant cousins, I would not be able to stand here if not for their sacrifices and support.

I would like to thank my grandmother, for providing her unconditional optimism and support. Her confidence in my ability to succeed gave me something to strive for, and motivated me throughout the toughest challenges of my degree.

Finally, I'd like to thank my mother, for always believing in me and encouraging me to pursue my dreams. From working long hours to provide for my brother and I growing up, to driving across the country to make sure I had access to the best opportunities possible, I could not have accomplished my work with her support.

DEDICATION

To my loving mother, Catherine Lorenzo.

Contents

List of Figures

List of Tables

Chapter 1

Introduction

1.1 Overview

In this thesis, we review the process of fabricating and designing a quadcopter platform weighing less than three grams.

1.2 Background

In today's society, drones have many practical applications, ranging from environmental surveying to package delivery. Among drones, the lightest and smallest hover, as do the smallest insects and birds. This allows them to maneuver though confined spaces and land easily. The key limitation of small hovering drones are limited battery life of <30 minutes, and their impact hazard for humans.

Hovering robots weighing less than a few grams, however, have the potential to mitigate these risks as collision offers a lower injury potential than with traditional drone platforms. Favorable scaling physics may allow very small robots to fly indefinitely in direct sunlight.[2, 3] They also are able to navigate complex air spaces, and sustain minimal damage to themselves in the event of a collision or fall. We propose TinyQuad, an ultra-lightweight quadrotor platform to realize this potential, as well as to aid in testing sensors and power methods for insect-inspired robots.

TinyQuad will also address a need for a more convenient testbed for technologies aimed at much smaller, approximately 200 mg flapping wing robots. Flapping wing robots, while robust in enduring hits, often have

short usage spans [4]. This short usage time combined with the extended time needed to train an individual to fabricate these robots results in considerable turn around times for applications or designs reliant on these platforms.

1.3 Challenges

Some challenges when approaching a platform of this scale include power management, chassis fabrication, and communication or control. Even the smallest lithium polymer batteries are a mass of 450mg [5], [6]. Additionally, the smallest prior flying robot platforms relied strictly on tethered flight, or difficult to use photovoltaic cells requiring tracking with a high-powered laser. When utilizing motors, limited mobility is available on the smallest flying robot platform piccolisimo, weighing 2.48 grams or 4.47 grams for its more maneuverable version [7].

1.4 Approach

We employ concepts from flying insect robot fabrication as well as traditional quadrotor control concepts to demonstrate the feasibility of TinyQuad's design. Through utilizing circuits etched into flexible PCB material we achieve a lightweight and compact form factor and we achieve rigidity by designing a carbon fiber airframe. We also utilize the smallest commercially available lithium polymer batteries to achieve the lowest possible self-powered quadcopter mass.

We implement a PD controller to achieve a stable hover in simulation, deriving velocity and angle from acceleration using methods shown in 4. The controller is structured with an inner loop which controls the quadcopter's angle, and an exterior loop which controls the quadcopter's lateral movement.

1.5 Outline

We will go over example cases for TinyQuad, theories behind TinyQuad's development, the design and implementation of TinyQuad, evaluation of TinyQuad's performance, and conclude with discussion and future directions.

Chapter 2

Extended Example

In this chapter we discus several proposed applications for the designed quadcopter, including testing of small sensors, power management investigations, and environmental monitoring. This establishes the significance of the project.

2.1 Environmental Monitoring

When paired with solar power harvesting, the lightweight nature of this platform offers the potential for an indefinite flight time, allowing for extended environmental monitoring. [3] This quadcopter is small in size, and offers a considerable maneuverability beyond what can currently be achieved by small-scale flapping wing insect robots. This allows for movement in and around branches, pipes, or other cluttered air spaces.

The small size of this quadcopter also allows for a reduced noise factor and aerial presence. When monitoring wildlife via a UAV, they may be startled or otherwise frightened by the noises produced by a drone of traditional scale [8]. This makes overhead observation of natural behaviors and population evaluation difficult. With the lower noise produced by this quadcopter in comparison to other alternative UAVs.

Even if collision were to happen, because of the quadcopter's small scale, damage to both the environment and the quadcopter would be minimal. And should the quadcopter be lost during operation, because of its small scale and low-cost components, fabrication of a replacement quadcopter can be done quickly.

2.2 Sensor Testing

Establishment of a performance baseline is critical for understanding how small sensors behave onboard flapping wing insect robots. Sensors such as optic flow, temperature, and Air Quality Index (AQI) sensors need to have a ground truth verification for performance onboard a flying robotic platform. [9]

Traditional flying insect robots have a limited carrying capacity (typically approximately 100 grams) [10]. This low carrying capacity combined with the short usage time of flying insect robots make extended testing runs difficult. Having a robust platform with sufficiently large carrying capacity ensures ample flight time to allow for adequate testing.

2.3 Power System Testing

Power is an issue of utmost concern when designing lightweight insect robots. Even the smallest commercially manufactured lithium polymer batteries weigh approximately 450mg, which can be too much for a 75mg robot to carry. This quadcopter offers a new way to test methods of powering small-scale robots such as small-scale photovoltaic cells, and RF harvesting.

Chapter 3

Theory

3.1 Introduction to Theory

In this section we discuss the pre-existing theories and groundwork that allowed for electronic design, controller design, and fabrication of the quadcopter.

3.2 Electronics Concept

We utilize the motor controller design provided by crazyflie's schematics, and motors were sourced from small-scale model airplane component manufacturers. The lightweight form factor was accomplished via DPSS rastering of flex PCB material.

Leads consisting of 43 gauge copper wire were hand-soldered to provide a connection point for evaluation of PWM modulation. Components were soldered on via the usage of solder paste and a hot plate, acting in place of a reflow oven. The enviornment's air quality was preserved by running a filter next to the hot plate at all times while in use.

3.3 Controller Concept

Quadcopter behavior previously has been evaluated using the viscoelastic control law, allowing for approximation as a mass attached to a spring. [11]

We evaluated the performance of both analog and digital controller approaches for the purpose of trajectory tracking. We elected to employ a standard PD controller to achieve a desired trajectory in simulation. We utilize the behaviors observed by the larger autonomous quadcopter Crazyflie and approximate this behavior at a smaller scale through the analogous form factor of the two platforms.

3.4 Chassis Concept

The fabrication of the chassis drew inspiration from traditional quadcopter layouts, and throughout the iteration process employed concepts found in foldable robotics. The process of creating a foldable carbon fiber assembly consists of cutting 2 pieces of carbon fiber to fit a specified shape. These shapes are then layered with a pyralux adhesive and kapton to ensure the ability to bend and fold about castelated joints.

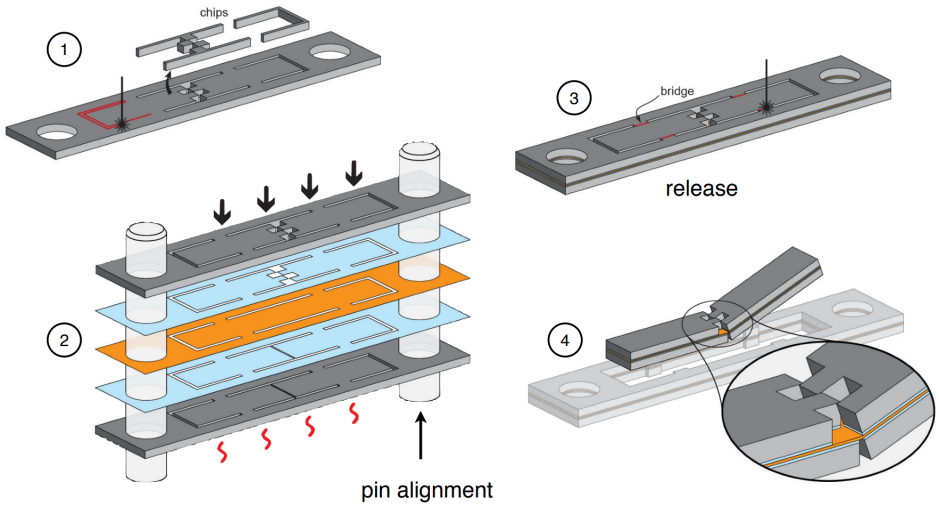

Figure 3.1: An example of folding robotics principles employed for the purpose of fabricating a foldable joint. Step one consists of cutting out an appropriately designed piece of carbon fiber with a DPSS laser, with castellated hinges placed to allow for folds without interference. In step 2 the light blue sheets of pyralux adhesive are layered with the orange sheet of kapton and our previously cut carbon fiber before being placed in a heat press to cure. Step 3 consists of utilizing the previously used DPSS laser to sever the cured layup from the excess carbon fiber used for alignment. The final step 4 illustrates the castellated joint allowing the pieces to bend and meet at a right angle without collision. Provided by [1].

Chapter 4

Design

4.1 Controller Design

Our proposed control architecture consists of cascaded control loops. An inner PD controller regulates attitude to a desired value. An outer loop PD controller regulates x position. It is designed assuming a temporal separation: that the inner loop's response time is negligibly fast compare to the outer loop 4.1.

4.1.1 Analog PD Controller

The PD Controller was further elaborated upon by utilizing a pre-existing simulation of the crazyflie operating using a PD controller.[12] The below matrix was employed to characterize the reduced scale system. The system was approximated by first utilizing a ratio of the crazyflie's mass and dimensionality to the new system's mass and dimensionality. The values used in calculation and their origin are provided in Table 4.1. Values for inertia about the x- and y- axes were derived from scaling existing estimates of crazyflie inertial values by $4md^2$, while values for inertia about the z axis were calculated by scaling crazyflie estimates by $4m(d\sqrt{2})^2$. Distance d was measured on the exterior perimeter of the quadcopter between the center points of two motors, and mass m was approximated with a 3 gram cutoff.

The J matrix arranges the calculated inertial values of the quadcopter in an accessible fashion. Being diagonal, it allows independent control of the aircraft's pitch and roll axes.

Variable	Quantity Represented	Numerical Value	Units
m	mass	3	g
d	length of quadcopter frame	0.015	m
J_{xx}	inertia of the quadcopter about the x axis	0.0027	kgm^2
J_{yy}	inertia of the quadcopter about the y axis	0.0027	kgm^2
J_{zz}	inertia of the quadcopter about the z axis	0.0054	kgm^2

Table 4.1: The meaning of the symbols used in the PD controller's calculations and their origin

$$J = \begin{bmatrix} J_{xx} & 0 & 0 \\ 0 & J_{yy} & 0 \\ 0 & 0 & J_{zz} \end{bmatrix}$$

We employ two PD controllers, with an interior loop following a desired theta to achieve a desired attitude, and an exterior loop which regulates lateral movement.

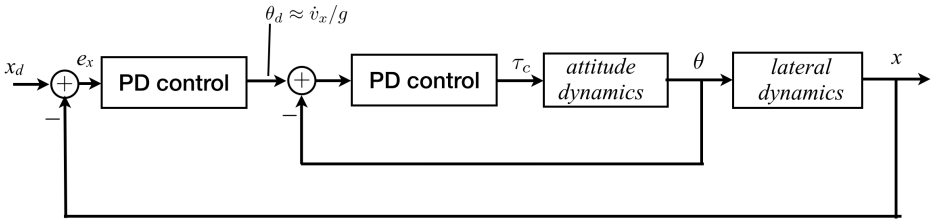

Figure 4.1: The block diagram of the proposed simulated controller.

We first derive the transfer function for the inner loop of the controller shown here, which accepts θ_d a desired θ and outputs a final θ. We assume our PD controller receives as input the error in θ, $e_\theta = \theta_d - \theta$. Its differential equation is given by

$$\tau_y = k_p e_\theta + k_d \dot{e_\theta}$$

To derive the transfer function, we assume that both τ_y and e_θ have the form of an exponential. This admits e.g. sinusoids, decaying sinusoids, and step signals as possible functions.

$$\tau_y(t) = Ae^{st}$$

$$e_\theta(t) = Be^{st}$$

$$\dot{e_\theta}(t) = sBe^{st}$$

$$Ae^{st} = k_pBe^{st} + k_dsBe^{st}$$

The controller's transfer function is the ratio of output to input:

$$C(s) = \frac{A}{B} = \frac{\tau}{e_\theta} = k_p + k_ds$$

Torque balance, which equates the angular acceleration to the sum of the torques being applied (via Newton's second law) results in a differential equation $\tau = J_{yy}\ddot{\theta}$. The corresponding transfer function of the plant is:

$$P(s) = \frac{1}{Js^2} = \frac{\theta}{\tau}$$

Resulting in final transfer function of the inner closed loop:

$$G(s) = \frac{C(s)P(s)}{1 + C(s)P(s)}$$

$$G(s) = \frac{k_ds + k_p}{J_{yy}s^2 + k_ds + k_p}$$

This then allows the system's response to be found using its natural frequency ω_n and damping ratio ζ via the process

$$2\zeta\omega_n = \frac{k_d}{J_{yy}}$$

$$\omega_n = \sqrt{\frac{k_p}{J}}$$

The gains k_p and k_d can then be selected to satisfy a desired rise time T_r via the formula $\omega_n = \frac{1.8}{T_r\zeta}$.

The desired damping ratio was calculated using the desired 2 percent overshoot and the below formula:

$$\zeta = \frac{\ln(\frac{\%OS}{100})}{\sqrt{\pi^2 + \ln(\frac{\%OS}{100})}}$$

When shaping the outer loop, we first describe our plant $P_o(s)$ by assuming an $x(t)$ and $\theta(t)$ as $x(t)$ is

also exponential in nature:

$$x(t) = Xe^{st}$$

$$\dot{x}(t) = sXe^{st}$$

$$\ddot{x}(t) = s^2Xe^{st}$$

$$\theta(t) = \Theta e^{st}$$

The lateral force on a drone in flight is approximately $mg\sin(\theta)$, assuming lift balances weight. Linearizing for small angles, the force balance is

$$\sum f_x = mg\theta = m\ddot{x}$$

Which for our context can also be written as

$$\ddot{x} = g\theta$$

Which is our differential equation. The second order transfer function is

$$\frac{X}{\Theta} = \frac{g}{s^2}$$

We assume a fast inner loop and then derive the exterior loop's plant P_o.

$$P_o = \frac{\Theta(s)}{F_x(s)} \cdot \frac{X}{\Theta(s)} = \frac{1}{mg} \cdot \frac{g}{s^2} = \frac{1}{ms^2}$$

4.1.2 Digital Controller

We also considered a digital implementation of control of z position, which is an independent control loop. The system was modelled as a mass-spring-damper approximation, where z is the quadcopter's altitude[11].

Following a similar derivation as above, its input-output dynamics are represented by the equation

$$Z(s) = k\frac{\omega_n^2}{s^2 + 2\zeta\omega_n s + \omega_n^2}\left[F_z(s)\right]$$

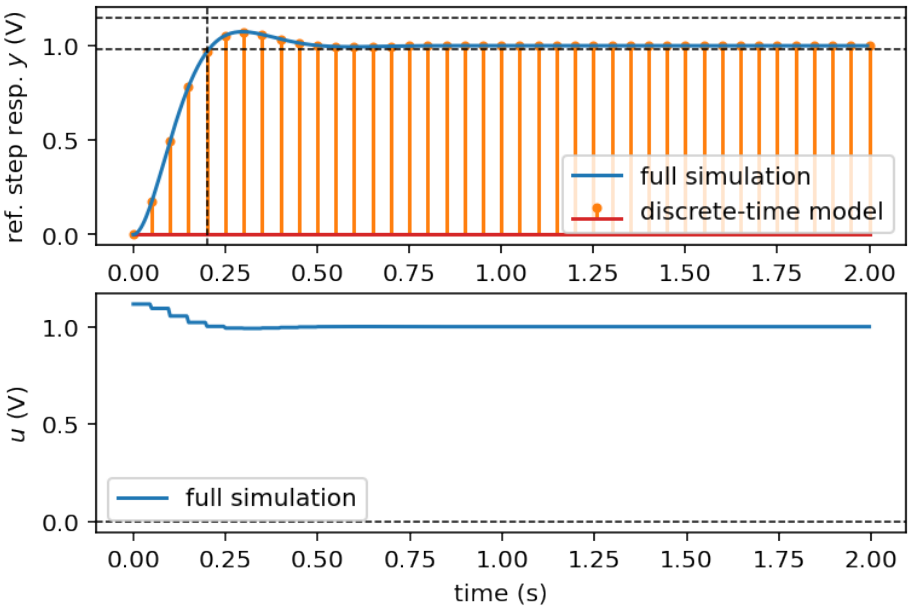

Figure 4.2: Simulated result of the digital controller's step response. Here our performance benchmarks are met, demonstrating the feasibility of this controller.

After calculation of the system's state space form, Matlab's SISO tool was used to calculate the desirable k_p and k_d gains to allow for appropriate and stable performance.

The simulation's step response was then produced to verify reasonable performance (Figure 4.2).

4.2 Motor Controller Circuit Design

Motor Controller circuit design was largely completed via the existing crazyflie schematics[13]. Some pulldown and additional safety resistors were modified to account for our circuit's lower power consumption requirements (4.3). The largest constraint in circuit design was the maximum possible current provided by the battery. A continuous issue in small-scale robotics is minimizing battery mass while still achieving sufficient motor lift. This has previously been solved via additional batteries, however with the advancement and size reduction of motors intended for usage in flying vehicles [14] we are less limited by this constraint. Positioning was evaluated using an acrylic mockup of the chassis (4.4).

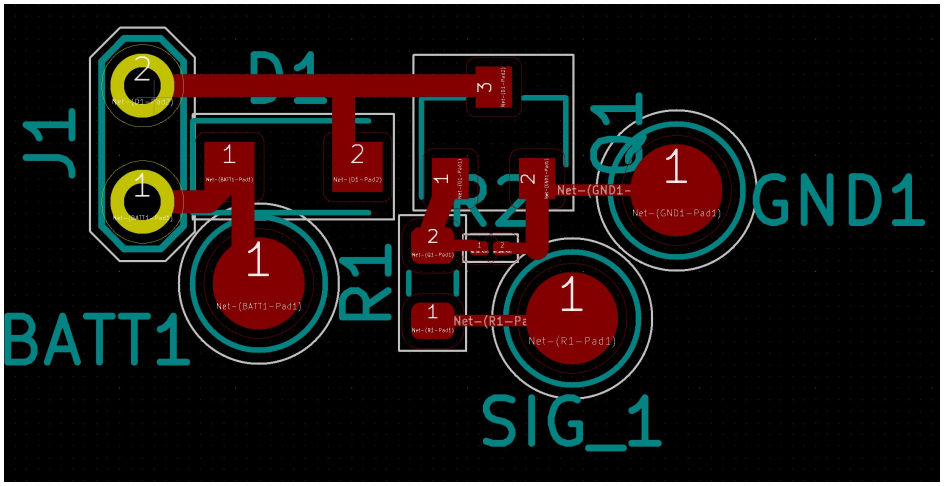

Figure 4.3: The most recent revision of the motor controller.

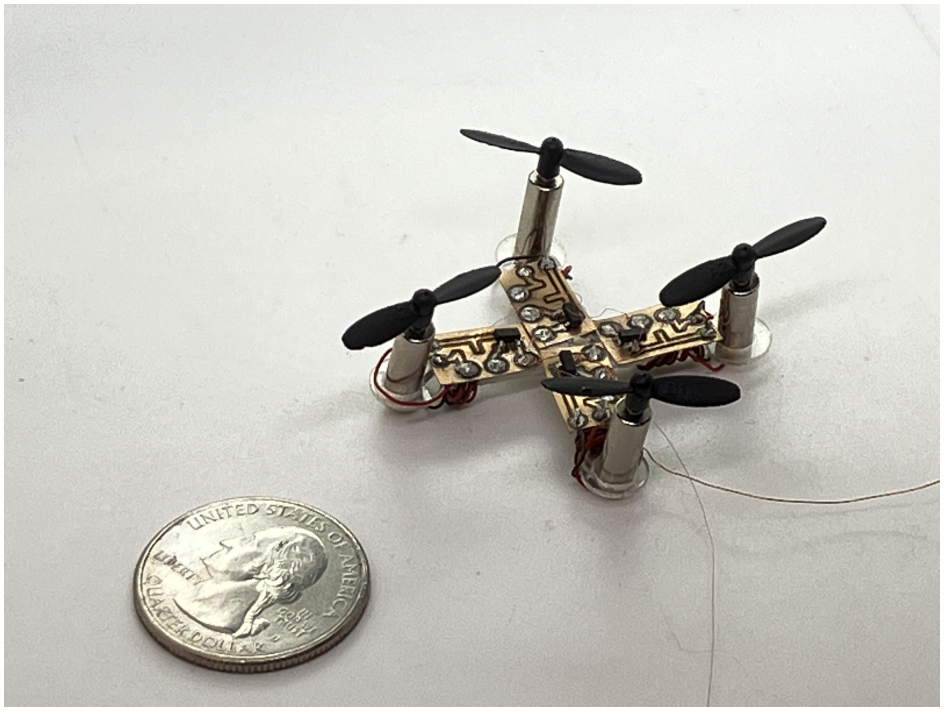

Figure 4.4: The acrylic version of the chassis used to evaluate motor and motor controller positioning.

4.3 Chassis Design

The quadrotor chassis is fabricated using a carbon fiber layup. Approaches which utilized origami style joints to form interlocking box-beams (4.8) were experimented with, but ultimately forgone in the interest of employing a simpler approach which did not rely as heavily on large-scale laser cutting operations. In reducing the reliance on larger scale cuts and reverting back to a simplistic, the amount of time needed to not only complete the initial cuts, but also return the assembly to the heatpress to be finalized. This also has the added effect of reducing the chassis's final mass.

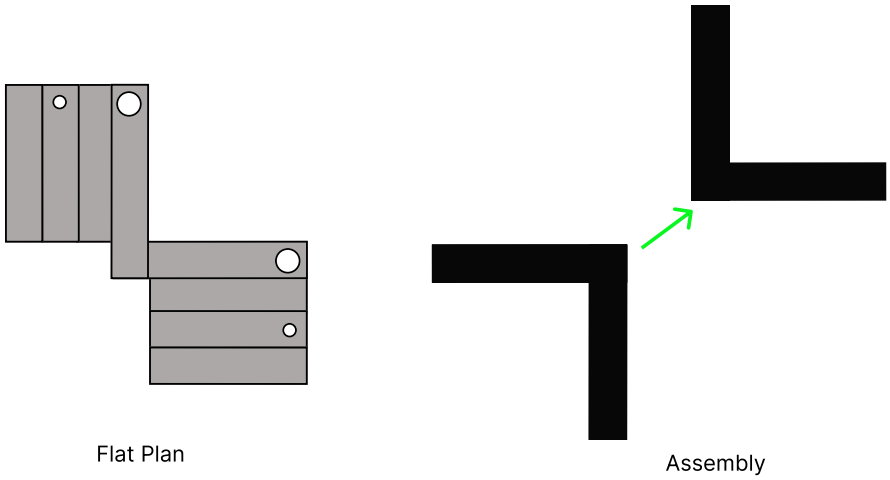

Figure 4.5: An example of the flat assembly and two of the flat assemblies being combined to form a single quadcopter frame.

One of the main constraints of chassis design was minimizing potential for propellers to collide with each other while the quadcopter was fabricated, as well as to minimize conflicting ground effects felt at the end of each arm during operation. In order to do so the diameter of the provided propellers was measured and and an additional radius provided to ensure no collision would occur.

The employed layup utilizes 3 layers of carbon fiber stacked in a 0-90-0 orientation, which has shown to provide optimal stiffness for function. [15] A single piece was cut four times from this layup, and the right corner of a glass slide used for alignment. The four pieces were then glued to each other using a central pad. Motors were glued directly to the frame. In preliminary testing, no significant adverse vibrational modes were observed in this approach. We employ the assembly technique seen in 4.7

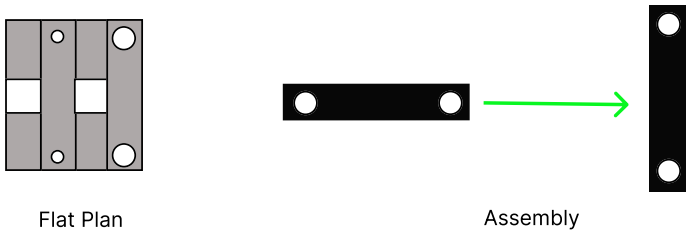

Figure 4.6: An alternate approach to the technique examined in 4.5. Here the beams interlock via the square shaped hole in the middle.

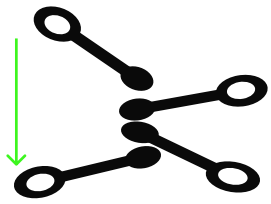

Figure 4.7: The assembly process of the finalized chassis. Four identical arms of the frame are glued at a right angle to each other. This approach eliminates the need for a second pass through the heat press, drastically reducing manufacturing time.

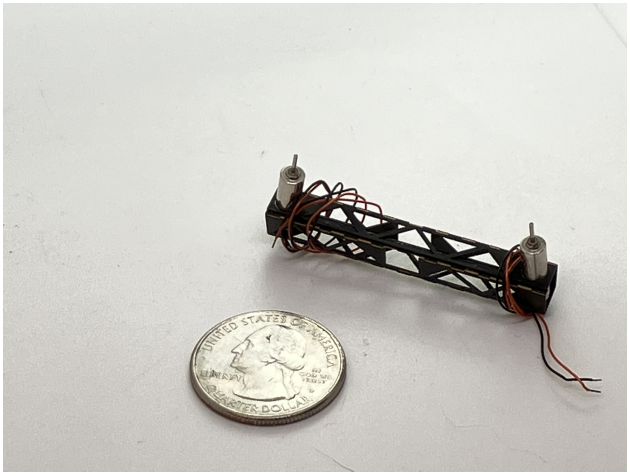

Figure 4.8: A test assembly utilizing origami-style folding techniques. Technically challenging to manufacture, this design was ultimately forgone.

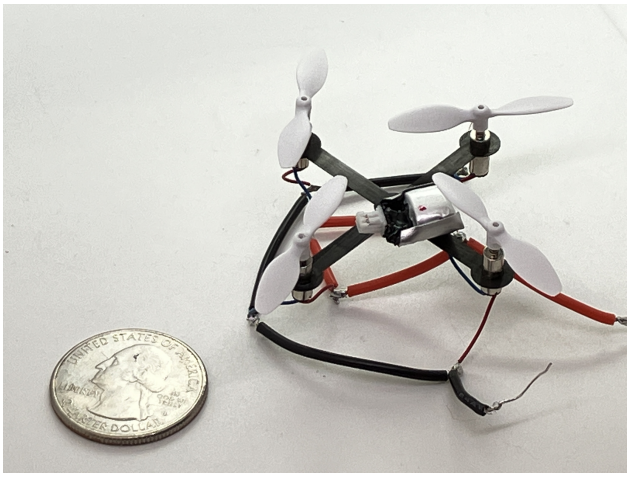

Figure 4.9: The finalized chassis layup. Motors are glued directly to the frame.

Chapter 5

Evaluation

5.1 Evaluation Methods

The primary methods of evaluation pertained to quadcopter motor performance and the mass of the quadcopter. This was due to the key criterion of the project being the lowest possible mass of the quadcopter.

5.2 Motor Performance

Thrust is evaluated by varying current to the motors while they are attached to a pair of reverse acting tweezers that are adhered to a balance. Motors are positioned an extensive distance away from any obstructions below them, so as to avoid incorrect readings due to ground effects. Final evaluations to verify all motors were capable of providing sufficient thrust when connected to the smallest possible battery occurred with all four proposed motors directly connected to the battery via a common bus line.

Approaches to quantify motor performance include a cantilevered attachment to a small scale, and connection to a multimeter to evaluate current draw in response to a provided PWM cycle. Because motors at this small scale traditionally are a part of small airplane design and fabrication, aside from their current draw very little information tends to be offered about their technical capabilities.

Thrust, being dependent upon propeller length and surface area, was highly subjective across evaluated motors. In addition to small-scale motors having limited technical information, their props are difficult to fabricate in a laboratory setting, and must be precisely fitted to the motor's shaft.

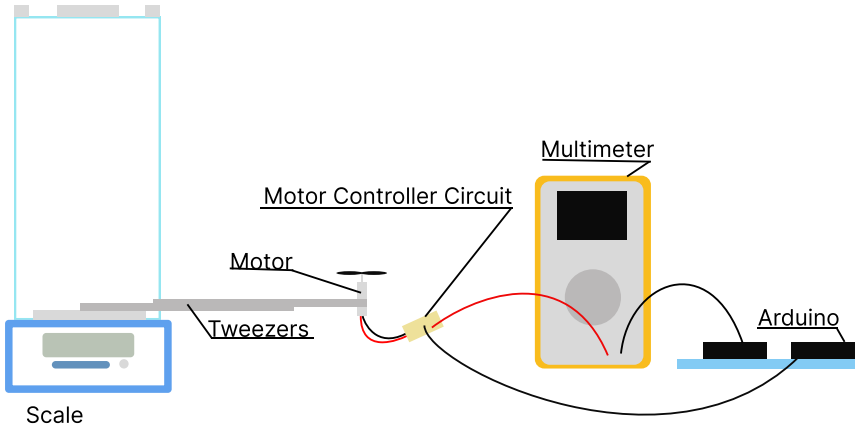

Figure 5.1: The test setup to evaluate the motor performance. This was used to determine the orientation of the motors, propeller fit, and maximum possible thrust/associated current draw.

Trial	1	2	3	Average
Observed Thrust (g)	2.9877	3.0046	2.9269	2.9731

Table 5.1: Thrusts provided by the 3x9mm motors during testing. Observed thrust exceeded mass.

Motor performance was evaluated using the setup shown in Figure 5.1. The PWM duty cycle was modulated using a potentiometer to verify that all circuits were functional and capable of responding to a provided signal.

Motor lift of a 4x12mm motor was evaluated in Figure 5.2 and efficiency was additionally evaluated in Figure 5.3.

To determine if the smallest grade commercial motors were capable of producing sufficient lift, all four motors were connected to a common bus line, and powered directly from the battery. With a direct battery connection, all four motors produced an average lift of 2.9731 grams. This excess lift capacity provides sufficient evidence to suggest that flight with this platform and an additional experimental payload of sensors or power systems is possible.

5.3 Mass Evaluation

Mass was evaluated using a Mettler Toledo analytical balance. Components were weighed individually and an average of individual kinds of off-the shelf components were taken. The balance was re-calibrated and

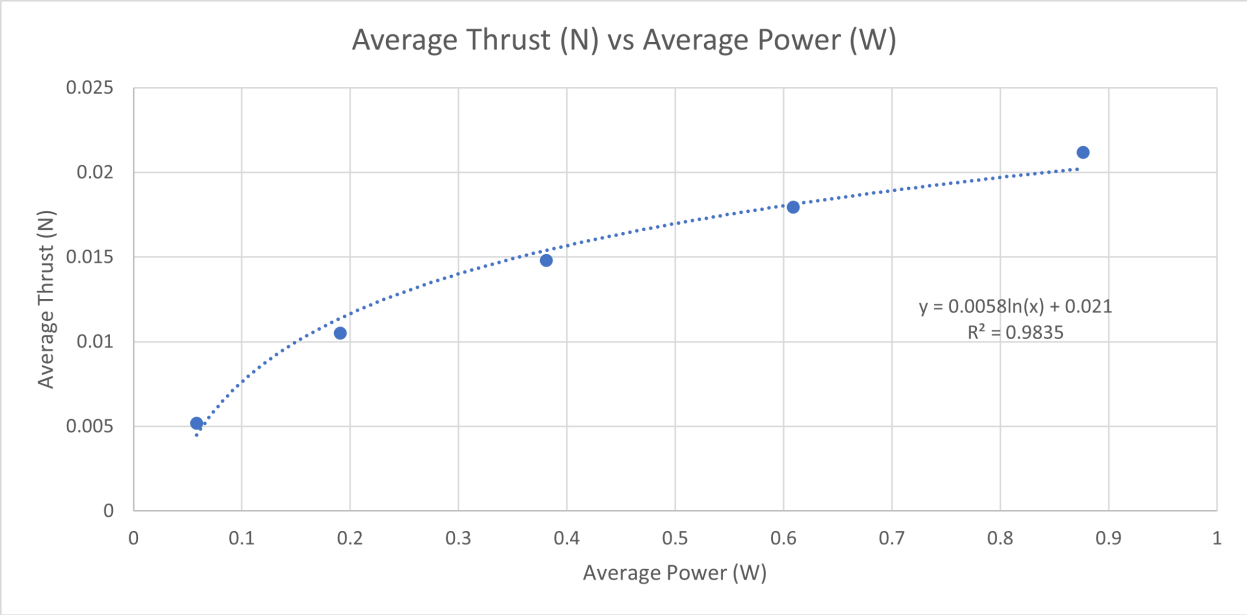

Figure 5.2: Graph of observed thrust vs power of a 4x12mm motor. The observed trend here is consistent with larger scale quadcopter brushless motor performance, which suggests sufficient performance of the motor controller.

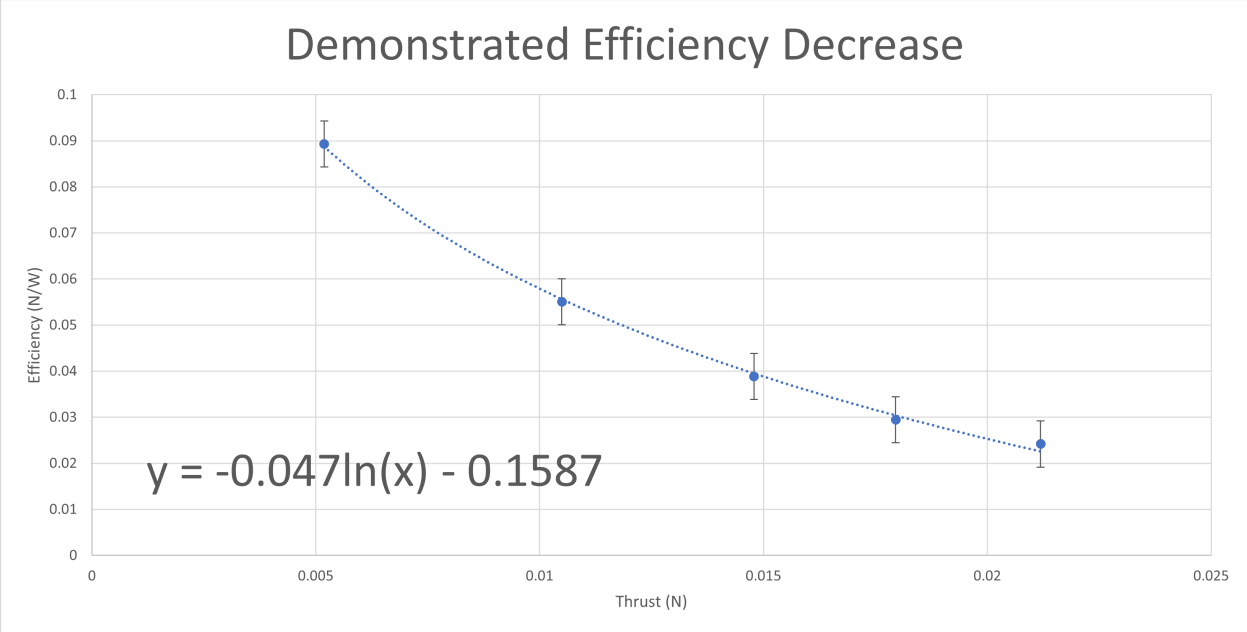

Figure 5.3: A graph correlating the motor's efficiency vs the observed thrust.

zeroed before every measurement. The mass of each component is outlined below in table 5.2.

Component	Mass (g)
Carbon Fiber Chassis	0.093
Motor (x4)	0.380
Battery	0.791
Motor Controller	0.094
Proposed Integration with Small Sensor Suite	0.187
NRF52 Chip	0.025
Total	2.710

Table 5.2: Mass of proposed components.

Combining the evaluated mass observed across all validated components with the observed possible lift, it is suggested that flight with these components is possible.

5.4 Controller Evaluation

Controller evaluation consisted of utilizing the proposed controller to fly to a predetermined target in a 2D plane. An example of this simulation is shown in Figure 5.4. Successful flight and utilization of this controller suggests that the quadrotor platform is capable of controlled lateral flight to a specified point, which exceeds prior controllability at this scale [7].

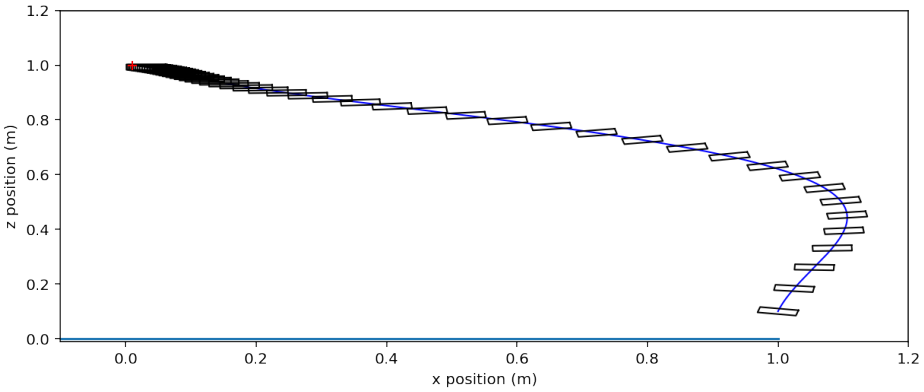

Figure 5.4: A graph of the simulated behavior of the quadcopter using the PD controller.

Chapter 6

Conclusion

6.1 Conclusion

In this work we presented a method of designing a lightweight quadrotor platform for testing and validating lightweight sensor and power design choices for flying insect robots.

A carbon fiber chassis was designed which allowed for fast, lightweight, and simple fabrication. Multiple approaches of varying complexity were examined, with the final approach of four paddle-shaped pieces of carbon fiber glued at perpendicular angles being selected for the final quadcopter. This finalized frame represents a transition from an approximately 2-3 hour fabrication time for our most complex frames to approximately 1.5 hours for our simplest frame.

After analyzing behavior and quantifying outputs of motor controllers, an equation was derived for determining performance in response to provided current, which was then used to estimate necessary battery size.

TinyQuad's viability was demonstrated by achieving lift for its estimated mass carrying the smallest commercially manufactured lithium polymer battery. All four of the smallest commercially available motors were connected directly to a lithium polymer battery, and the produced thrust exceeded the final calculated quadcopter mass.

In simulation the proposed controller was able to reach a proposed target altitude and maintain stability. This was done using the PD controller outlined in Chapter 4, which was tuned using the proposed mass

cutoffs for the final small quadcopter.

This represents a reduction of approximately 10x the mass of the lightest commercially available autonomous quadcopter. Alternative flying micro aerial vehicles of similar scale lack either the onboard autonomy potential, or the potential maneuverability offered by a quadcopter's form factor.

6.2 Future Work

Integration with a lightweight IMU onboard will allow for position stabilization without needing to be tethered to a power source/heavier controller. Currently the mass of the battery is heavier than strictly necessary due to the MCX connector attached that is necessary for safe interfacing with the battery. Utilizing a magnetic connector would serve to continue to provide this safe interface option, but with reduced mass compared to the battery's current MCX plug.

Additionally, with the advent of position stabilization, it is expected traditional quadcopter maneuverability will follow, allowing for controlled flights and communication via bluetooth.

Bibliography

[1] Sawyer Fuller, "Foldable Robotics," 2018.

[2] N. Elkunchwar, S. Chandrasekaran, V. Iyer, and S. B. Fuller, "Toward battery-free flight: Duty cycled recharging of small drones," in *2021 IEEE/RSJ International Conference on Intelligent Robots and Systems (IROS)*, pp. 5234–5241, Sept. 2021. ISSN: 2153-0866.

[3] M. Qi, "Sunlight-powered hovering of an ultra-light micro aerial vehicle," Feb. 2024. ISSN: 2693-5015.

[4] Y. M. Chukewad, J. James, A. Singh, and S. Fuller, "RoboFly: An Insect-Sized Robot With Simplified Fabrication That Is Capable of Flight, Ground, and Water Surface Locomotion," *IEEE Transactions on Robotics*, vol. 37, pp. 2025–2040, Dec. 2021. Conference Name: IEEE Transactions on Robotics.

[5] B. Diouf and R. Pode, "Potential of lithium-ion batteries in renewable energy," *Renewable Energy*, vol. 76, pp. 375–380, Apr. 2015.

[6] C. Depcik, T. Cassady, B. Collicott, S. P. Burugupally, X. Li, S. S. Alam, J. R. Arandia, and J. Hobeck, "Comparison of lithium ion Batteries, hydrogen fueled combustion Engines, and a hydrogen fuel cell in powering a small Unmanned Aerial Vehicle," *Energy Conversion and Management*, vol. 207, p. 112514, Mar. 2020.

[7] M. Piccoli and M. Yim, "Piccolissimo: The smallest micro aerial vehicle," in *2017 IEEE International Conference on Robotics and Automation (ICRA)*, pp. 3328–3333, May 2017.

[8] F. Christiansen, L. Rojano-Doñate, P. T. Madsen, and L. Bejder, "Noise Levels of Multi-Rotor Un-

manned Aerial Vehicles with Implications for Potential Underwater Impacts on Marine Mammals," *Frontiers in Marine Science*, vol. 3, Dec. 2016. Publisher: Frontiers.

[9] K. K. Lekkala and V. K. Mittal, "Accurate and augmented navigation for quadcopter based on multi-sensor fusion," in *2016 IEEE Annual India Conference (INDICON)*, pp. 1–6, Dec. 2016. ISSN: 2325-9418.

[10] Y. P. Talwekar, A. Adie, V. Iyer, and S. B. Fuller, "Towards Sensor Autonomy in Sub-Gram Flying Insect Robots: A Lightweight and Power-Efficient Avionics System," in *2022 International Conference on Robotics and Automation (ICRA)*, pp. 9675–9681, May 2022.

[11] M. K. Sahoo, J. K. Dutt, and S. K. Saha, "Quadcopter control using the viscoelastic control law," in *2021 21st International Conference on Control, Automation and Systems (ICCAS)*, pp. 539–543, Oct. 2021. ISSN: 2642-3901.

[12] Sawyer Fuller, "me586_2d_crazyflie_simulator_pd," 2022.

[13] Bitcraze AB, "Crazyflie 2.1," Dec. 2018.

[14] V. Kumar and N. Michael, "Opportunities and Challenges with Autonomous Micro Aerial Vehicles," in *Robotics Research : The 15th International Symposium ISRR* (H. I. Christensen and O. Khatib, eds.), pp. 41–58, Cham: Springer International Publishing, 2017.

[15] Q. Zhang, J. Chen, L. Yang, W. Dong, X. Sheng, and X. Zhu, "Structure Optimization and Implementation of a Lightweight Sandwiched Quadcopter," in *Intelligent Robotics and Applications* (H. Liu, N. Kubota, X. Zhu, and R. Dillmann, eds.), (Cham), pp. 220–229, Springer International Publishing, 2015.

Chapter A

Component Masses

Mass (g)	Capacity (mAh)
0.450	10
0.720	20
0.900	30

Table A.1: Battery Masses and Currents

Mass (g)	Thrust (g)
0.380	0.743
0.800	2.160

Table A.2: Motor Masses and Observed Thrusts

Chapter B

Glossary

AQI	Air Quality Index
MAV	Micro Aerial Vehicle
Quadcopter	A flying aerial robot which uses four symmetrically motors to achieve lift. Also known colloquially as a drone.
Airframe	Rigid piece of material used to hold Quadcopter components in a fixed orientation and distance to each other. Used interchangeably with frame and chassis.
Origami Robotics	A set of techniques and design choices which employ traditional origami folds as either a part of robot fabrication or robot actuation.
PWM	Pulse Width Modulation
DPSS Laser	Diode Pumped Solid State Laser
IMU	Inertial Measurement Unit, sensor package consisting of positional sensors such as accelerometers and gyroscopes
UAV	Unmanned Aerial Vehicle